First-Principles-Driven Model-Based Optimal Control of the Current Profile in NSTX-U

Zeki Ilhan[1], Justin Barton[1], William Wehner[1], Eugenio Schuster[1], David Gates[2], Stefan Gerhardt[2], Egemen Kolemen[2], Jonathan Menard[2]

[1]Department of Mechanical Engineering & Mechanics
Lehigh University

[2]Princeton Plasma Physics Laboratory

zoi210@lehigh.edu

56th Annual Meeting of the APS Division of Plasma Physics

October 29, 2014

Motivation for Current Profile Control in NSTX-U

- Some of the next-step operational goals for NSTX-Upgrade include [1]:
  - Non-inductive sustainment of the high-β spherical torus.
  - High performance equilibrium scenarios with neutral beam heating.
  - Longer pulse durations.
- **Active, model-based, feedback control** of the **current profile** evolution can be useful to achieve those stability and performance criteria.
- The ***q*-profile**, which is related to the **toroidal current density** in the machine, plays an important role in the stability and performance of a given magnetic configuration.
- Availability of the additional neutral beam current sources ***enables feedback control of the current profile*** in NSTX-U.

[1] GERHARDT, S. P. et al., Nuclear Fusion (2012).

Model-based Feedback Control Scheme

- ***Modeling for control design and not for physical understanding!***
- **The control-oriented model** only needs to **capture the dominant effects** of the actuators on the current profile evolution.
- Control-oriented model is **embedded in current-profile controller**.

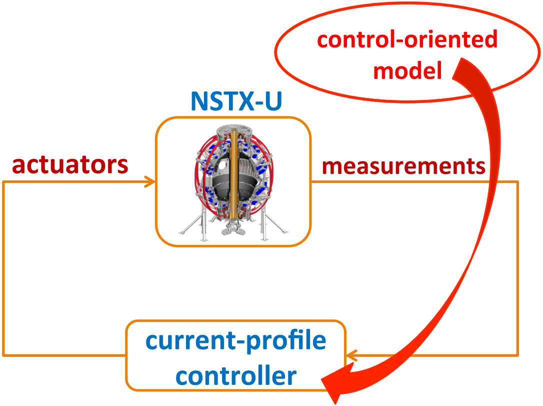

First-Principles-Driven (FPD) Current Profile Modeling

Physics–based Empirical Models for: T_e , n_e , η , j_{NI}	$+$	Poloidal Flux Evolution Model (Magnetic Diffusion Equation)

First – Principles – Driven (FPD) Current Profile Evolution Model

- The evolution of the poloidal magnetic flux is given by [2]:

$$\boxed{\frac{\partial \psi}{\partial t} = \frac{\eta(T_e)}{\mu_0 \rho_b^2 \hat{F}^2} \frac{1}{\hat{\rho}} \frac{\partial}{\partial \hat{\rho}} \left(\hat{\rho} D_\psi \frac{\partial \psi}{\partial \hat{\rho}} \right) + R_0 \hat{H} \eta(T_e) \frac{\langle \bar{j}_{ni} \cdot \bar{B} \rangle}{B_{\phi,0}}} \tag{1}$$

with boundary conditions

$$\left. \frac{\partial \psi}{\partial \hat{\rho}} \right|_{\hat{\rho}=0} = 0 \qquad \left. \frac{\partial \psi}{\partial \hat{\rho}} \right|_{\hat{\rho}=1} = -\frac{\mu_0}{2\pi} \frac{R_0}{\hat{G}\big|_{\hat{\rho}=1} \hat{H}\big|_{\hat{\rho}=1}} I(t), \tag{2}$$

where $D_\psi(\hat{\rho}) = \hat{F}(\hat{\rho})\hat{G}(\hat{\rho})\hat{H}(\hat{\rho})$, and $\hat{F}$, $\hat{G}$, $\hat{H}$ are geometric factors pertaining to the magnetic configuration of a particular plasma equilibrium.

[2] OU, Y., et al., Fusion Engineering and Design (2007).

First-Principles-Driven (FPD) Current Profile Modeling

- NSTX-U-tailored [3] empirical models [4] for the electron temperature, electron density, plasma resistivity, and noninductive current drives [5] takes the form

$$n_e(\hat{\rho},t) = n_e^{prof}(\hat{\rho})u_n(t) \tag{3}$$

$$T_e(\hat{\rho},t) = k_{T_e}(\hat{\rho},t_r)\frac{T_e^{prof}(\hat{\rho},t_r)}{n_e(\hat{\rho},t)}I(t)\sqrt{P_{tot}(t)} \tag{4}$$

$$\eta(T_e) = \frac{k_{sp}(\hat{\rho},t_r)Z_{eff}}{T_e(\hat{\rho},t)^{3/2}} \tag{5}$$

$$\begin{aligned}\frac{\left\langle \bar{j}_{ni}\cdot\bar{B}\right\rangle}{B_{\phi,0}} &= \sum_{i=1}^{6}\frac{\left\langle \bar{j}_{nbi_i}\cdot\bar{B}\right\rangle}{B_{\phi,0}} + \frac{\left\langle \bar{j}_{bs}\cdot\bar{B}\right\rangle}{B_{\phi,0}} \\ &= \sum_{i=1}^{6} k_i^{prof}(\hat{\rho})j_i^{dep}(\hat{\rho})\frac{\sqrt{T_e(\hat{\rho},t)}}{n_e(\hat{\rho},t)}P_i(t) \\ &+ \frac{k_{JeV}R_0}{\hat{F}(\hat{\rho})}\left(\frac{\partial\psi}{\partial\hat{\rho}}\right)^{-1}\left[2\mathcal{L}_{31}T_e\frac{\partial n_e}{\partial\hat{\rho}} + \{2\mathcal{L}_{31}+\mathcal{L}_{32}+\alpha\mathcal{L}_{34}\}n_e\frac{\partial T_e}{\partial\hat{\rho}}\right]\end{aligned} \tag{6}$$

[3] ILHAN, Z. O. et al., 55th Annual Meeting of the APS DPP (2013)
[4] BARTON, J. E. et al., 52nd IEEE CDC (2013)
[5] SAUTER, O. et al., Physics of Plasmas (1999), (2002)

FPD Model Tailoring for NSTX-U Run 121123R42

- **NOTE: NSTX-U run 121123R42 is a TRANSP run with the NSTX-U shape and actuators, using the scaled profiles from NSTX.**

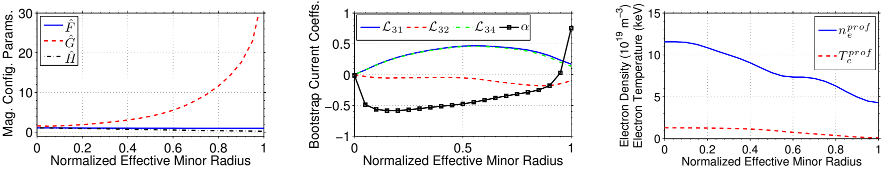

(a) $\hat{F}(\hat{\rho}), \hat{G}(\hat{\rho}), \hat{H}(\hat{\rho})$ (b) $\mathcal{L}_{31}(\hat{\rho}), \mathcal{L}_{32}(\hat{\rho}), \mathcal{L}_{34}(\hat{\rho}), \alpha(\hat{\rho})$ (c) $n_e^{prof}(\hat{\rho}), T_e^{prof}(\hat{\rho})$

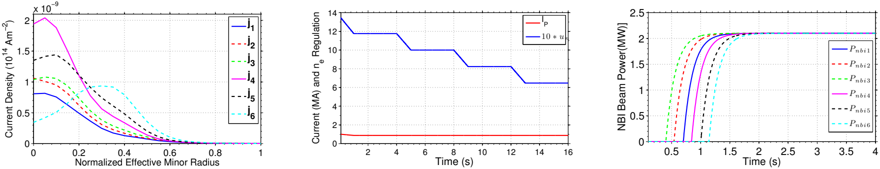

(d) NB deposition profiles (e) Current and n_e regulation (f) NB injection powers

Fig. 1: Reference (a) magnetic configuration parameters, (b) bootstrap current coefficients, (c) electron density and temperature profiles. (d) Individual NB deposition profiles. Inputs: (e) plasma current and n_e regulation, (f) NB injection powers (constant after 4s.)

- **Poloidal Flux Profile Comparison - $\psi(\hat{\rho})$, at fixed time**

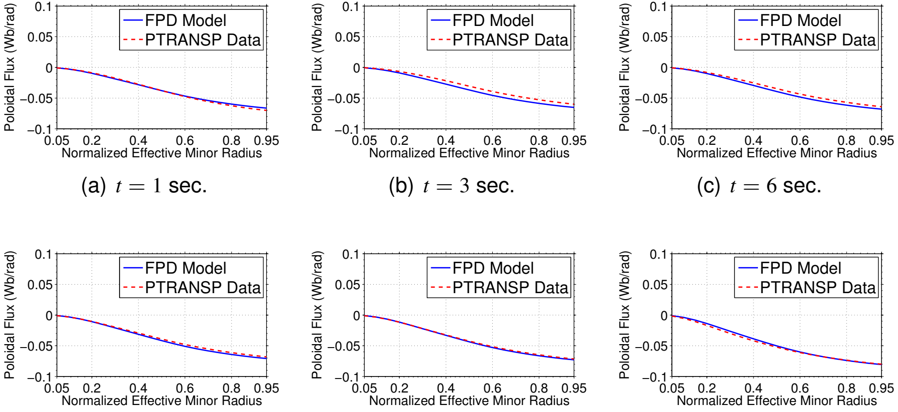

(a) $t = 1$ sec. (b) $t = 3$ sec. (c) $t = 6$ sec.

(d) $t = 9$ sec. (e) $t = 12$ sec. (f) $t = 15$ sec.

Fig. 2: Poloidal magnetic flux profile evolution comparison.

FPD Model Tailoring for NSTX-U Run 121123R42

- **Safety Factor Profile Comparison - $q(\hat{\rho})$, at fixed time**

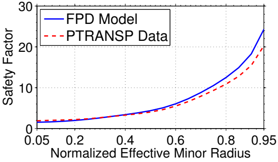

(a) $t = 1$ sec.

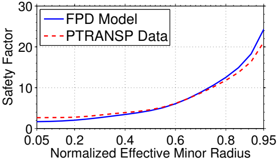

(b) $t = 3$ sec.

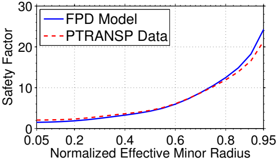

(c) $t = 6$ sec.

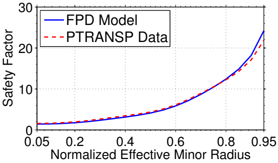

(d) $t = 9$ sec.

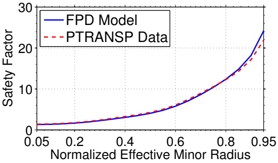

(e) $t = 12$ sec.

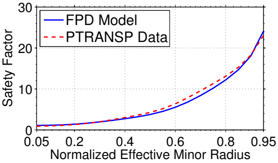

(f) $t = 15$ sec.

Fig. 3: Safety factor profile evolution comparison.

FPD Model Validation for NSTX-U Run 121123N80

- The **FPD model tailored** based on the NSTX-U TRANSP run **121123R42** is **simulated** using the **inputs** and the **geometry** of the NSTX-U TRANSP run **121123N80.**

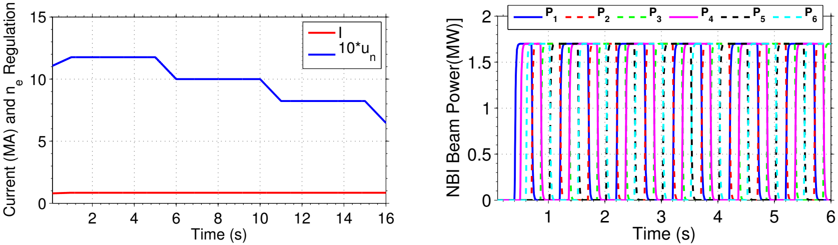

(a) Plasma current and n_e regulation

(b) Individual NBI beam powers

Fig. 4: Control inputs extracted from NSTX-U TRANSP run 121123N80: (a) Plasma current and n_e regulation, (b) NB injection powers (same trend continues after 6s.)

- **Poloidal Flux Profile Comparison - $\psi(\hat{\rho})$, at fixed time**

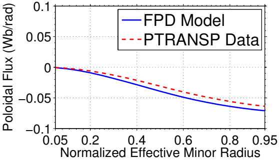

(a) $t = 1$ sec.

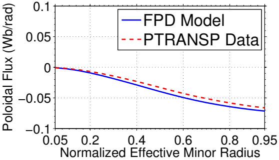

(b) $t = 3$ sec.

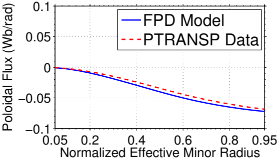

(c) $t = 6$ sec.

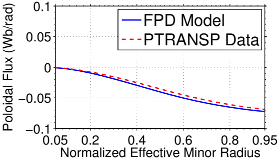

(d) $t = 9$ sec.

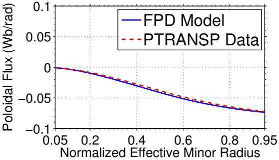

(e) $t = 12$ sec.

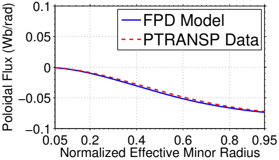

(f) $t = 15$ sec.

Fig. 5: Poloidal magnetic flux profile evolution comparison.

FPD Model Validation for NSTX-U Run 121123N80

- **Safety Factor Profile Comparison - $q(\hat{\rho})$, at fixed time**

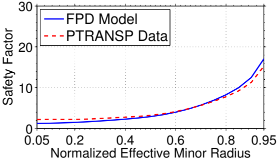

(a) $t = 1$ sec.

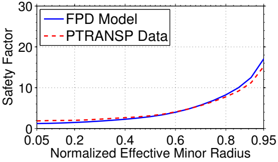

(b) $t = 3$ sec.

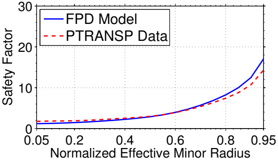

(c) $t = 6$ sec.

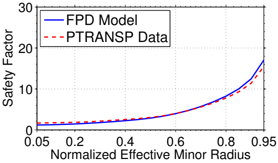

(d) $t = 9$ sec.

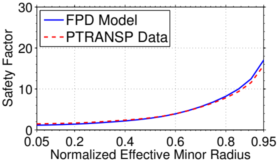

(e) $t = 12$ sec.

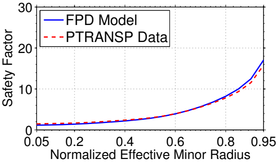

(f) $t = 15$ sec.

Fig. 6: Safety factor profile evolution comparison.

FPD Model in Control-Oriented Form

- By substituting the simplified scenario-oriented models for the electron density (3), electron temperature (4), plasma resistivity (5), and noninductive current drives (6) into the magnetic diffusion equation (1)-(2), space and time functions can be separated.
- As a result, the magnetic diffusion equation takes the form

$$\boxed{\frac{\partial\psi}{\partial t} = f_\eta(\hat\rho)u_\eta(t)\frac{1}{\hat\rho}\frac{\partial}{\partial\hat\rho}\left(\hat\rho D_\psi(\hat\rho)\frac{\partial\psi}{\partial\hat\rho}\right) + \sum_{i=1}^{6} f_i(\hat\rho)u_i(t) + f_{bs}(\hat\rho)u_{bs}(t)\left(\frac{\partial\psi}{\partial\hat\rho}\right)^{-1}} \tag{7}$$

where the boundary conditions become

$$\left.\frac{\partial\psi}{\partial\hat\rho}\right|_{\hat\rho=0} = 0, \quad \left.\frac{\partial\psi}{\partial\hat\rho}\right|_{\hat\rho=1} = -f_b u_b(t), \tag{8}$$

where

$$f_b = \frac{\mu_0}{2\pi}\frac{R_0}{\hat G\big|_{\hat\rho=1}\hat H\big|_{\hat\rho=1}} \tag{9}$$

$$u_b(t) = I(t)$$

FPD Model in Control-Oriented Form

- Spatial functions appearing compactly in (7) can be expressed in terms of various plasma model reference profiles and constants as

$$f_\eta(\hat{\rho}) = \frac{k_{sp}(\hat{\rho}) Z_{eff} n_e^{prof}(\hat{\rho})^{3/2}}{\mu_0 \rho_b^2 \hat{F}(\hat{\rho})^2 k_{T_e}(\hat{\rho})^{3/2} T_e^{prof}(\hat{\rho})^{3/2}} \tag{10}$$

$$D_\psi(\hat{\rho}) = \hat{F}(\hat{\rho}) \hat{G}(\hat{\rho}) \hat{H}(\hat{\rho}) \tag{11}$$

$$f_i(\hat{\rho}) = R_0 \hat{H}(\hat{\rho}) k_i^{prof}(\hat{\rho}) j_i^{dep}(\hat{\rho}) \frac{k_{T_e}(\hat{\rho})^{1/2} T_e^{prof}(\hat{\rho})^{1/2}}{n_e^{prof}(\hat{\rho})^{3/2}} \quad (i = 1, 2, ..., 6) \tag{12}$$

$$\begin{aligned} f_{bs}(\hat{\rho}) = {} & R_0 \hat{H}(\hat{\rho}) \frac{k_{JeV} R_0}{\hat{F}(\hat{\rho})} \left[2\mathcal{L}_{31} \frac{dn_e^{prof}(\hat{\rho})}{d\hat{\rho}} \frac{k_{sp}(\hat{\rho}) Z_{eff} n_e^{prof}(\hat{\rho})^{1/2}}{k_{T_e}(\hat{\rho})^{1/2} T_e^{prof}(\hat{\rho})^{1/2}} \ldots \right. \\ & \left. + \{2\mathcal{L}_{31} + \mathcal{L}_{32} + \alpha \mathcal{L}_{34}\} \frac{d}{d\hat{\rho}} \left\{ \frac{k_{T_e}(\hat{\rho}) T_e^{prof}(\hat{\rho})}{n_e^{prof}(\hat{\rho})} \right\} \frac{k_{sp}(\hat{\rho}) Z_{eff} n_e^{prof}(\hat{\rho})^{5/2}}{k_{T_e}(\hat{\rho})^{3/2} T_e^{prof}(\hat{\rho})^{3/2}} \right] \end{aligned} \tag{13}$$

FPD Model in Control-Oriented Form

- Time functions appearing compactly in (7) are nonlinear functions of the physical inputs:

$$u_\eta(t) = \frac{u_n(t)^{3/2}}{I(t)^{3/2} P_{tot}(t)^{3/4}} \tag{14}$$

$$u_i(t) = \frac{P_i(t)}{I(t)\sqrt{P_{tot}(t)}} \quad (i = 1, 2, ..., 6) \tag{15}$$

$$u_{bs}(t) = \frac{u_n(t)^{3/2}}{I(t)^{1/2} P_{tot}(t)^{1/4}} \tag{16}$$

$$u_b(t) = I(t), \tag{17}$$

  where $P_{tot}(t) = \sum_{i=1}^{6} P_i(t)$.

- Equations (14)-(17) are the outputs of the profile controller (the so-called "*control inputs*" for the numerical simulations).

FPD Model in Control-Oriented Form

- The safety factor $q(\hat{\rho},t) = -d\Phi/d\Psi(\hat{\rho},t)$ can be used to specify the toroidal current density. Using $\Phi = \pi B_{\phi,0}\rho^2$ and $\hat{\rho} = \rho/\rho_b$, the q-profile is expressed as:
$$q(\hat{\rho},t) = \frac{1}{\bar{\iota}} = -\frac{d\Phi}{d\Psi} = -\frac{d\Phi}{2\pi d\psi} = -\frac{\frac{\partial\Phi}{\partial\rho}\frac{\partial\rho}{\partial\hat{\rho}}}{2\pi\frac{\partial\psi}{\partial\hat{\rho}}} = -\frac{B_{\phi,0}\rho_b^2\hat{\rho}}{\partial\psi/\partial\hat{\rho}} \tag{18}$$
- Since the safety factor q depends inversely on the poloidal flux gradient, it is possible to define
$$\theta(\hat{\rho},t) = \frac{\partial\psi}{\partial\hat{\rho}} \tag{19}$$
as the ***to-be-controlled variable.***
- Substituting the *to-be-controlled variable* $\theta(\hat{\rho},t) = \frac{\partial\psi}{\partial\rho}$ into (7),
$$\frac{\partial\psi}{\partial t} = f_\eta u_\eta \frac{1}{\hat{\rho}}\left(\hat{\rho}D_\psi'\theta + D_\psi\theta + \hat{\rho}D_\psi\theta'\right) + \sum_{i=1}^{6} f_i u_i + f_{bs}u_{bs}\theta^{-1}, \tag{20}$$
where $(.)' = \partial/\partial\hat{\rho}$ for simplicity. Also, note that the time and space dependencies are dropped to reduce the representation.
- By differentiating (20) wrt $\hat{\rho}$, the PDE governing the evolution of the *to-be-controlled variable* $\theta(\hat{\rho},t)$ can be obtained.

Model Reduction via Spatial Discretization

- The PDE governing the evolution of the ***to-be-controlled variable*** $\theta(\hat{\rho}, t)$ can be expressed compactly as

$$\boxed{\frac{\partial \theta}{\partial t} = h_0(\hat{\rho}) u_\eta \theta'' + h_1(\hat{\rho}) u_\eta \theta' + h_2(\hat{\rho}) u_\eta \theta + f_{bs}' \frac{1}{\theta} u_{bs} - f_{bs} \frac{\theta'}{\theta^2} u_{bs} + \sum_{i=1}^{6} f_i' u_i}, \tag{21}$$

  subject to the boundary conditions

$$\theta\Big|_{\hat{\rho}=0} = 0, \qquad \theta\Big|_{\hat{\rho}=1} = -f_b u_b(t), \tag{22}$$

- The governing PDE (21) is discretized in space into l nodes using the truncated Taylor series approach while leaving the time domain continuous. The discrete form of (21) yields

$$\boxed{\dot{\boldsymbol{\theta}}(t) = \boldsymbol{g}(\boldsymbol{\theta}(t), \boldsymbol{u}(t))} \tag{23}$$

- $\boldsymbol{\theta} = [\theta_2, \theta_3, ..., \theta_{l-1}]^T \in \mathbb{R}^{(l-2)\times 1}$ is the value of $\theta(\hat{\rho}, t)$ at the $n = l - 2$ interior nodes (i.e., "*states*").
- $\boldsymbol{u} = [u_\eta, u_1, u_2, ..., u_6, u_{bs}, u_b]^T \in \mathbb{R}^{9\times 1}$ is the input vector
- $\boldsymbol{g} \in \mathbb{R}^{(l-2)\times 1}$ is a **nonlinear vector function** of the states, inputs and the model parameters.

Model Linearization

$$\boxed{\dot{\boldsymbol{\theta}}(t) = \boldsymbol{g}(\boldsymbol{\theta}(t), \boldsymbol{u}(t))} \tag{24}$$

- Let $\boldsymbol{\theta}_{ff}(t)$ and $\boldsymbol{u}_{ff}(t)$ define a set of feedforward values of the system states and inputs satisfying

$$\dot{\boldsymbol{\theta}}_{ff} = \boldsymbol{g}(\boldsymbol{\theta}_{ff}, \boldsymbol{u}_{ff}) \tag{25}$$

- To obtain a model suitable for control design, the following perturbation values are defined:

$$\Delta\boldsymbol{\theta}(t) = \boldsymbol{\theta}(t) - \boldsymbol{\theta}_{ff}(t) \tag{26}$$

$$\Delta\boldsymbol{u}(t) = \boldsymbol{u}(t) - \boldsymbol{u}_{ff}(t), \tag{27}$$

- Equation (24) can be expanded around the desired feedforward state and input vectors by using first order Taylor series approximation

$$\dot{\boldsymbol{\theta}} = \boldsymbol{g}(\boldsymbol{\theta}_{ff}, \boldsymbol{u}_{ff}) + \left.\frac{\partial \boldsymbol{g}}{\partial \boldsymbol{\theta}}\right|_{\boldsymbol{\theta}_{ff}, \boldsymbol{u}_{ff}} (\boldsymbol{\theta} - \boldsymbol{\theta}_{ff}) + \left.\frac{\partial \boldsymbol{g}}{\partial \boldsymbol{u}}\right|_{\boldsymbol{\theta}_{ff}, \boldsymbol{u}_{ff}} (\boldsymbol{u} - \boldsymbol{u}_{ff}) \tag{28}$$

$$\Delta\dot{\boldsymbol{\theta}} + \dot{\boldsymbol{\theta}}_{ff} = \boldsymbol{g}(\boldsymbol{\theta}_{ff}, \boldsymbol{u}_{ff}) + \left.\frac{\partial \boldsymbol{g}}{\partial \boldsymbol{\theta}}\right|_{\boldsymbol{\theta}_{ff}, \boldsymbol{u}_{ff}} \Delta\boldsymbol{\theta}(t) + \left.\frac{\partial \boldsymbol{g}}{\partial \boldsymbol{u}}\right|_{\boldsymbol{\theta}_{ff}, \boldsymbol{u}_{ff}} \Delta\boldsymbol{u}(t) \tag{29}$$

Linear-Time-Variant (LTV) Model for the Perturbation Values

$$\boxed{\Delta\dot{\boldsymbol{\theta}}(t) = A(t)\Delta\boldsymbol{\theta}(t) + B(t)\Delta\boldsymbol{u}(t)}, \tag{30}$$

where

$$A(t) = \left.\frac{\partial \mathbf{g}}{\partial \boldsymbol{\theta}}\right|_{\boldsymbol{\theta}_{ff}(t),\boldsymbol{u}_{ff}(t)} \in \mathbb{R}^{(l-2)\times(l-2)} \tag{31}$$

$$B(t) = \left.\frac{\partial \mathbf{g}}{\partial \boldsymbol{u}}\right|_{\boldsymbol{\theta}_{ff}(t),\boldsymbol{u}_{ff}(t)} \in \mathbb{R}^{(l-2)\times 9} \tag{32}$$

are the so-called "***system jacobians***".

- Equation (30) represents a linearized, state-space version of the nonlinear plasma response model around some predefined "*feedforward*" state and input trajectories, $\boldsymbol{\theta}_{ff}(t)$ and $\boldsymbol{u}_{ff}(t)$.

Control Objective

- The goal is to achieve desired safety factor values $\bar{q}$ (or, desired $\bar{\theta}$ values since $\bar{\theta}(\hat{\rho}, t) = -B_{\phi,0}\rho_b^2\hat{\rho}/\bar{q}(\hat{\rho}, t)$) at certain plasma radial locations.
- To select those radial locations where profile control is to be enforced, the *"output"* is modeled as $\boldsymbol{y}(t) = C\boldsymbol{\Delta\theta}(t)$, where $C \in \mathbb{R}^{m\times n}$ is the *"output matrix"* and $\boldsymbol{y}(t) \in \mathbb{R}^{m\times 1}$ is the output vector with $m = 9$ (number of control outputs chosen equal to the number of control inputs).
- The control objective is to make the output $\boldsymbol{y}(t)$ track a constant reference $\boldsymbol{z}$ *as closely as possible* during the time interval $[t_0, t_f]$ with *minimum control effort.* For this application, the tracking error, $\boldsymbol{e}(t) \in \mathbb{R}^{m\times 1}$, is defined as

$$\boldsymbol{e}(t) = \int_{t_0}^{t_f} [\boldsymbol{y}(\tau) - \boldsymbol{z}]\, d\tau \quad \Rightarrow \quad \dot{\boldsymbol{e}}(t) = \boldsymbol{y}(t) - \boldsymbol{z} = C\boldsymbol{\Delta\theta}(t) - \boldsymbol{z} \tag{33}$$

- In order to reject the disturbance and improve the tracking performance of the close-loop system, *integral action is required in the optimal control law.* This is achieved by defining an augmented state vector, $\widetilde{\boldsymbol{x}}$ as

$$\widetilde{\boldsymbol{x}}(t) = \left[\begin{array}{c} \boldsymbol{e}(t) \\ \hline \boldsymbol{\Delta\theta}(t) \end{array}\right] \tag{34}$$

Control Design

Linear Quadratic Integral (LQI) Optimal Controller Design

- The optimal control problem is stated with the following cost functional

$$\boxed{\min_{\boldsymbol{\Delta u}(t)} J = \frac{1}{2}\widetilde{\boldsymbol{x}}^T(t_f)\widetilde{P}(t_f)\widetilde{\boldsymbol{x}}(t_f) + \frac{1}{2}\int_{t_0}^{t_f}\left[\widetilde{\boldsymbol{x}}^T(t)\widetilde{Q}\widetilde{\boldsymbol{x}}(t) + \boldsymbol{\Delta u}^T(t)R\boldsymbol{\Delta u}(t)\right]dt} \quad (35)$$

subject to

$$\boxed{\dot{\widetilde{\boldsymbol{x}}}(t) = \widetilde{A}(t)\widetilde{\boldsymbol{x}}(t) + \widetilde{B}(t)\boldsymbol{\Delta u}(t)} \quad (36)$$

- Note that $\widetilde{Q}$ and R are symmetric and positive definite weight matrices and

$$\widetilde{A}(t) = \begin{bmatrix} 0_{m\times m} & C_{m\times n} \\ 0_{n\times m} & A(t)_{n\times n} \end{bmatrix}, \ \widetilde{B}(t) = \begin{bmatrix} 0_{m\times m} \\ B(t)_{n\times m} \end{bmatrix}. \quad (37)$$

- The solution of the optimization problem (35)-(36) yields an optimal solution for $\boldsymbol{\Delta u}(t)$ as

$$\boxed{\boldsymbol{\Delta u}(t) = -K_I(t)\int_{t_0}^{t_f}\left[C(\tau)\boldsymbol{\Delta\theta}(\tau) - \boldsymbol{z}\right]d\tau - K_P(t)\boldsymbol{\Delta\theta}(t),} \quad (38)$$

Closed-Loop Control Simulation Results

- Two different closed-loop control simulations are carried out utilizing the same feedforward inputs but different initial conditions and target profiles.
- Both feedforward $\theta_{ff}(\hat{\rho}, t)$ and target $\bar{\theta}(\hat{\rho}, t)$ state trajectories are generated by simulating the magnetic diffusion equation (MDE) with the physical inputs set to the following arbitrary constants:

	u_n	P_1 [MW]	P_2 [MW]	P_3 [MW]
Feedforward	0.7	0.1	0.4	0.7
Target (Case I)	1.0	0.5	0.7	0.9
Target (Case II)	0.9	0.3	0.8	0.8

	P_4 [MW]	P_5 [MW]	P_6 [MW]	I_p [MA]
Feedforward	1.0	1.3	1.1	0.5
Target (Case I)	1.1	1.1	1.5	0.7
Target (Case II)	1.3	0.9	1.2	0.9

- The reference profiles and constants of the control-oriented model are adopted based on the NSTX-U TRANSP run 121123R42.

Closed-Loop Control Simulation Results

CASE I

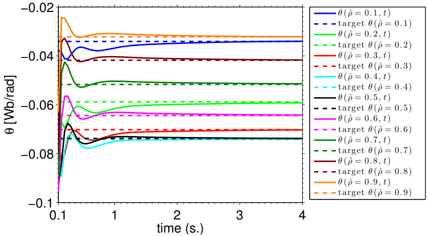

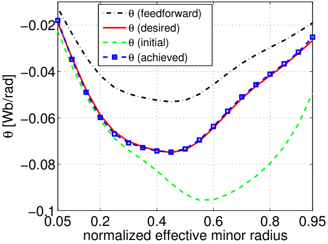

CASE II

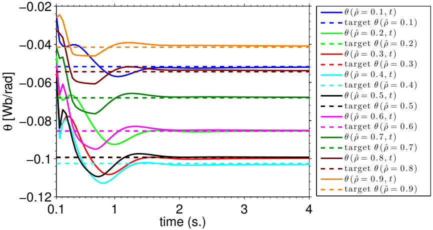

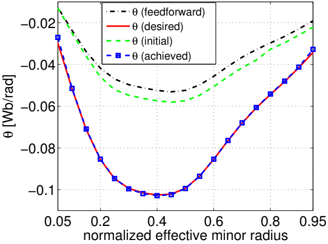

Figures (upper left & right): Time evolution of the optimal outputs (solid) with their respective targets (dashed).
Figures (lower left & right): Comparison of the initial, feedforward and desired $\theta(\hat\rho)$ profiles along with the profile achieved by feedforward+feedback control at $t = 2$ s.

CASE I

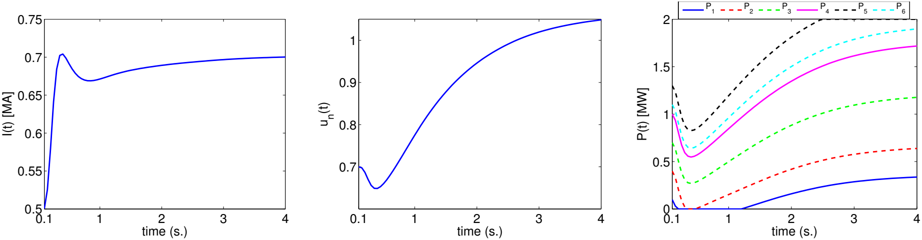

CASE II

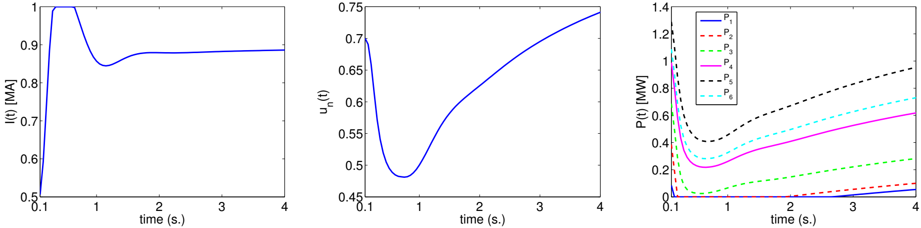

Figures: (left) Time evolution of the optimal plasma current, (center) time evolution of the optimal n_e regulation, and (right) time evolution of the optimal neutral beam injection powers.

Closed-Loop Control Simulation Results

CASE I

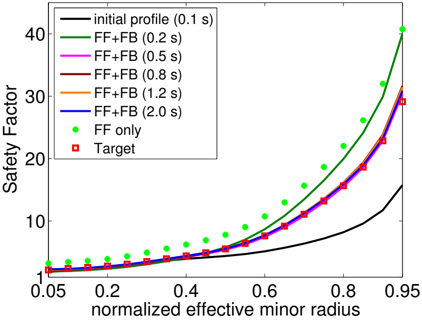

CASE II

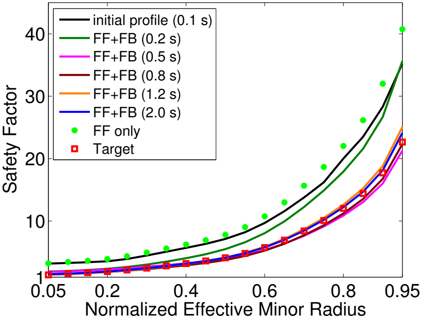

Figures (left & right): Time evolution of the safety factor profiles.

Closed-Loop Control Simulation Results

- **The same simulation as in case 1** is carried out, this time by turning the feedback off in between $2-3$ sec.
- **Time Evolution of the Optimal Outputs:**

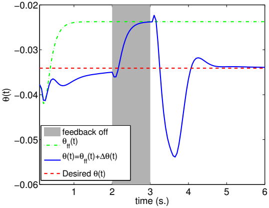

(a) $y_1 = \theta(\hat{\rho} = 0.1, t)$

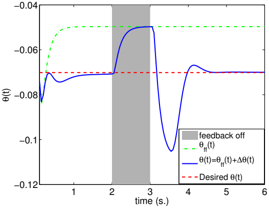

(b) $y_3 = \theta(\hat{\rho} = 0.3, t)$

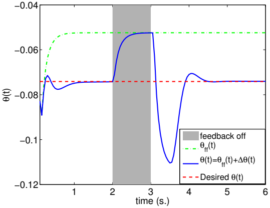

(c) $y_4 = \theta(\hat{\rho} = 0.4, t)$

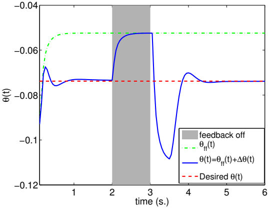

(d) $y_5 = \theta(\hat{\rho} = 0.5, t)$

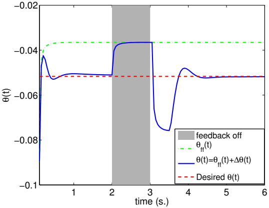

(e) $y_7 = \theta(\hat{\rho} = 0.7, t)$

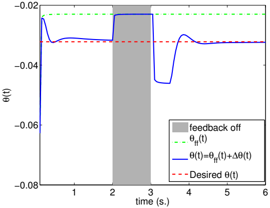

(f) $y_9 = \theta(\hat{\rho} = 0.9, t)$

Closed-Loop Control Simulation Results

- **Time Evolution of the Optimal Inputs:**

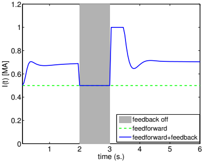

(a) $I(t)$

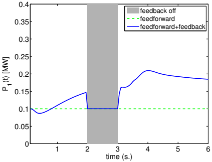

(b) $P_1(t)$

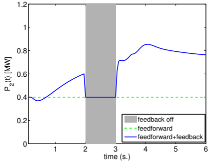

(c) $P_2(t)$

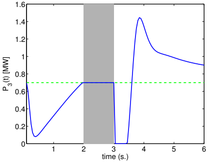

(d) $P_3(t)$

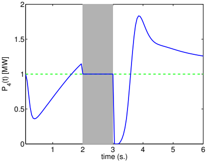

(e) $P_4(t)$

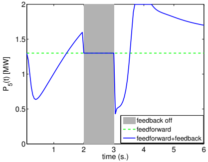

(f) $P_5(t)$

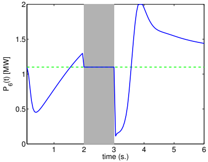

(g) $P_6(t)$

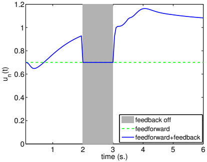

(h) $u_n(t)$

Figures: Time evolution of the optimal inputs

Conclusions

- An NSTX-U-tailored plasma response model is put into a control-oriented form and the resulting infinite-dimensional, nonlinear PDE is then reduced through spatial discretization by a truncated Taylor series expansion.
- The nonlinear, finite-dimensional model is linearized around feedforward state and input trajectories. In this way, a state-space LTV model is obtained describing the dynamics around the feedforward trajectories.
- An LQI feedback controller is designed based on this control-oriented, LTV model to regulate the poloidal flux gradient profile, and hence the current profile or the safety factor profile, around a desired target profile.
- The effectiveness of the proposed controller in shaping the poloidal flux gradient profile is tested in simulations based on the MDE solver.
- The next step is to test the controller in a TRANSP closed-loop simulation and then in experiments once NSTX-U starts operation.